PHARMACEUTICAL BIOLOGY
2024, VOL. 62, NO. 1, 1–12
https://doi.org/10.1080/13880209.2023.2289577

Taylor & Francis
Taylor & Francis Group

RESEARCH ARTICLE

Shenxiang Suhe pill improves cardiac function through modulating gut microbiota and serum metabolites in rats after acute myocardial infarction

Xinqin Zhong[a,b], Junyuan Yan[a,b], Xing Wei[a,b], Tian Xie[a,b], Zhaojian Zhang[a,b], Kaiyue Wang[a,b], Congying Sun[a,b], Wei Chen[c], Jiaming Zhu[c], Xin Zhao[a,b] and Xiaoying Wang[a,b,d]

[a]Ministry of Education Key Laboratory of Pharmacology of Traditional Chinese Medical Formulae, Tianjin University of Traditional Chinese Medicine, Tianjin, China; [b]State Key Laboratory of Component-based Chinese Medicine, Tianjin University of Traditional Chinese Medicine, Tianjin, China; [c]Hangzhou Hu Qing Yu Tang Pharmaceutical Co., Ltd, Hangzhou, China; [d]School of Chinese Materia Medica, Tianjin University of Traditional Chinese Medicine, Tianjin, China

ABSTRACT

Context: Shenxiang Suhe pill (SXSH), a traditional Chinese medicine, is clinically effective against coronary heart disease, but the mechanism of cardiac-protective function is unclear.

Objective: We investigated the cardiac-protective mechanism of SXSH *via* modulating gut microbiota and metabolite profiles.

Materials and methods: Sprague-Dawley (SD) male rats were randomly divided into 6 groups ($n=8$): Sham, Model, SXSH (Low, 0.063 g/kg; Medium, 0.126 g/kg; High, 0.252 g/kg), and Ato (atorvastatin, 20 mg/kg). Besides the Sham group, rats were modelled with acute myocardial infarction (AMI) by ligating the anterior descending branch of the left coronary artery (LAD). After 3, 7, 14 days' administration, ultrasound, H&E staining, serum enzymic assay, 16S rRNA sequencing were conducted to investigate the SXSH efficacy. Afterwards, five groups of rats: Sham, Model, Model-ABX (AMI with antibiotics-feeding), SXSH (0.126 g/kg), SXSH-ABX were administrated for 14 days to evaluate the gut microbiota-dependent SXSH efficacy, and serum untargeted metabolomics test was performed.

Results: 0.126 g/kg of SXSH intervention for 14 days increased ejection fraction (EF, 78.22%), fractional shortening (FS, 109.07%), and aortic valve flow velocities (AV, 21.62%), reduced lesion area, and decreased serum LDH (8.49%) and CK-MB (10.79%). Meanwhile, SXSH upregulated the abundance of Muribaculaceae (199.71%), *Allobaculum* (1744.09%), and downregulated *Lactobacillus* (65.51%). The cardiac-protective effect of SXSH was disrupted by antibiotics administration. SXSH altered serum metabolites levels, such as downregulation of 2-*n*-tetrahydrothiophenecarboxylic acid (THTC, 1.73%), and lysophosphatidylcholine (lysoPC, 4.61%).

Discussion and conclusion: The cardiac-protective effect and suggested mechanism of SXSH could provide a theoretical basis for expanding its application in clinic.

ARTICLE HISTORY
Received 12 January 2023
Revised 25 September 2023
Accepted 26 November 2023

KEYWORDS
Traditional Chinese medicine (TCM); muribaculaceae; *Allobaculum*; *Lactobacillus*; serum metabolic biomarker; 2-*n*-tetrahydrothio phenecarboxylic acid (THTC); lysophosphatidylcholine (lysoPC)

Introduction

Acute myocardial infarction (AMI), also known as ischemic heart disease, is myocardial necrosis caused by acute and persistent myocardial ischemia and hypoxia due to the interruption of coronary blood circulation (Nabel and Braunwald 2012). Although angioplasty, stenting and adjuvant drug therapy can open blocked coronary arteries and reduce the early mortality rate of AMI (Zijlstra 2000; Gelfand and Cannon 2007; Stone 2008), some patients still suffer from malignant ventricular remodeling due to excessive myocardial necrosis or impaired repair of the infarcted area, ultimately leading to heart failure or even death. New therapies are urgently needed to improve patient prognosis.

Alterations in the gut microbes and derived metabolites have been linked to changes in oxidant stress and inflammation and cardiovascular disease development. Gut microbiota-targeted therapies for coronary artery disease, and specific microbe and metabolite markers have been identified as subsequent clinical intervention targets. Patients with ST-segment elevation myocardial infarction (STEMI) presented gut microbial dysbiosis characterized by high relative abundance of Proteobacteria and Enterobacteriaceae. Moreover, systemic inflammation-associated microbial metabolites lipopolysaccharide (LPS) and D-lactate, and trimethylamine-*N*-oxide (TMAO) are increased during adverse cardiovascular events (Zhou et al. 2018; Kwun et al. 2020). Therefore, gut microbiota might be a potential preventive and therapeutic target for AMI.

Chinese medicines have been widely used for the clinical treatment of coronary heart disease for thousands of years (Wang C et al. 2018). Coronary heart disease is a physical and mental disease that originates in the heart and involves the five viscera, and the pathogenesis is paralysis of the heart veins, which belongs to the categories of 'thoracic obstruction' and 'cardialgia'

CONTACT Xin Zhao x.zhao26@tjutcm.edu.cn; Xiaoying Wang wxy@tjutcm.edu.cn Ministry of Education Key Laboratory of Pharmacology of Traditional Chinese Medical Formulae, Tianjin University of Traditional Chinese Medicine, 10 Poyanghu Road, Jinghai District, Tianjin 301617, China

(Gong et al. 2017). Shenxiang Suhe pill (SXSH) (Chinese Pharmacopoeia Commission 2020) originated from the Suhexiang pill in Volume 3 of the 'Prescriptions of the Bureau of Taiping People's Welfare Pharmacy', which is composed of 11 herbs, including *Moschus moschiferus* Linn. (Cervidae), *Cinnamomum camphora* (L.) Presl (Lauraceae), *Liquidambar orientalis* Mill. (Altingiaceae), *Styrax tonkinensis* (Pierre) Craib ex Hart. (Styracaceae), and *Cyperus rotundus* Linn. (Cyperaceae). SXSH is traditionally used for chest paralysis caused by cold invading the heart, resulting in an insufficient flow of Qi and blood. The symptoms are heart pain, chest tightness, aggravated by cold, coronary heart disease, and angina pectoris (Liu J et al. 2020; Shi et al. 2022; Wei et al. 2022). *Liquidambar orientalis* and *S. tonkinensis* regulate Qi to dissipate phlegm; *M. moschiferus* and *C. camphora* restore mental clarity and activate the meridian. *Boswellia carterii* Birdw. (Burseraceae), *Eugenia caryophllata* Thunb. (Myrtaceae), *Aucklandia lappa* Decne. (Compositae), *Aquilaria sinensis* (Lour.) Gilg (Thymelaeaceae) and *C. rotundus* are pungent, warm-natured drugs for activating Qi, lowering adverse Qi, and removing the obstruction of Qi and blood circulation to restore mental clarity. *Atractylodes macrocephala* Koidz. (Compositae) invigorates the spleen and stomach, and *Bubalus bubalis* Linn. (Bovidae) clears away heat and toxic materials. Therefore, SXSH is often used to treat coronary heart disease in clinics by regulating the flow of Qi and activating blood circulation.

Pharmacological studies have revealed that SXSH can relieve ventricular premature beat in coronary heart disease and prevent angina pectoris attacks by increasing coronary blood flow and reducing myocardial oxygen consumption (Chen et al. 2000; Zhu et al. 2016). Our previous study indicated that SXSH can modulate the gut microbiota by downregulating the abundance of Lachnospiraceae, Rikenellaceae, Prevotellaceae, *Streptococcus, Romboutsia,* and *Monoglobus,* and upregulating the abundance of *Lactococcus* and *Roseburia* in AMI rats (Wei et al. 2022). However, whether the gut microbiota play important roles in the therapeutic effects of SXSH on AMI remains unclear. In this study, we aim to elucidate the underlying mechanisms of SXSH in alleviating AMI by improving gut microbiota and metabolite profiles.

Materials and methods

Animals, modelling, and treatment

Six-week-old Sprague-Dawley (SD) male rats were purchased from Huafukang Animal Experiment Centre (Beijing, China). All the rats were housed in groups of 5 animals per cage in a controlled specific pathogen free (SPF) condition (22 ± 2 °C, 40–60% relative humidity) with 12 h light/dark cycle in the Animal Centre of Tianjin University of Traditional Chinese Medicine. Rats were conditioned to environment prior to beginning of the study and fed standard chow diet and water ad libitum. All the procedures on animals were in accordance with the Guidance Suggestions for the Care and Use of Laboratory Animals (Ministry of Science and Technology of China) and approved by the Laboratory Animal Ethics Committee of Tianjin University of Traditional Chinese Medicine (TCM-LAEC2018013).

To induce the model of AMI, occlusion of the left anterior descending coronary artery (LAD) was employed as previously reported (Forte et al. 2021). In brief, rats were anaesthetized with R520 mobile small animal anesthesia machine (Reward Life Technology Co., Ltd., Shenzhen, China). The skin, fat and muscle were gently separated and then the fourth intercostal space on the left side of the chest was exposed. The anterior descending branch of the coronary artery was ligated with 5/0 polypropylene sutures and the muscle and skin were closed with 2/0 polypropylene sutures respectively. In the Sham group, only the corresponding coronary artery was threaded without ligation.

After surgery, the experiment animals were randomly divided into groups ($n = 8$): (A) Sham group (without LAD), (B) Model group (with LAD), (C) positive drug atorvastatin-treated group (Ato, 20 mg/kg), (D) SXSH-treated groups [0.063 g/kg (Low), 0.126 g/kg (Medium), 0.252 g/kg (High)], (E) antibiotics-treated Model group (Model-ABX), and (F) antibiotics-treated SXSH groups (SXSH-ABX). Saline (Otsuka Pharmaceutical Co., Ltd., Tianjin, China), SXSH (National Drug Approval No. Z33020141, Hangzhou Hu Qing Yu Tang Pharmaceutical Co., Ltd., Hangzhou, China), and atorvastatin (Pfizer Pharmaceutical Co., Ltd., Dalian, China) were administered by oral gavage for 3, 7, 14 days, respectively. For *in vivo* antibiotic treatment, rats were treated with combined antibiotics (ABX) containing 62.5 μg/mL ampicillin, 62.5 μg/mL metronidazole, 62.5 μg/mL neomycin (Solarbio, Beijing, China), and 31.25 μg/mL vancomycin (Sigma Aldrich, St. Louis, MO, USA) in sterile water. ABX treatment was initiated 7 days before AMI surgery. All rats were sacrificed under the deeply anesthetized condition after echocardiographic examinations. The serum samples were collected for serum biochemical and untargeted metabolomics analysis. The heart tissues were obtained and then fixed in 10% formalin buffer for further study (Table 1).

Echocardiography

All rats were anesthetized with isoflurane (Reward Life Technology Co., Ltd., Shenzhen, China) at 0, 3, 7, 14 days after surgery. The cardiac function of rats was evaluated by echocardiography with a Vevo2100 Ultrasound system (Visual Sonics, Canada) equipped with an MS-250, 16.0–21.0 MHZ intraoperative probe as previously described (Zhuang et al. 2022). B- and M-mode ultrasound views about parasternal long-axis, parasternal short-axis and 2 apical four-chamber long-axis were obtained. The parameters such as left ventricular ejection fraction (EF) and fractional shortening (FS), and aortic valve flow velocities (AV) were recorded by measuring the systolic and diastolic phases in rats.

Histopathological analysis

The myocardial tissues were treated with different concentrations of ethanol, xylene, soft wax and hard wax, followed by

Table 1. Diagrammatic representation of groups.

Group	Intervention	Dose
Sham	Saline fed	–
Model	Saline fed	–
Ato	Atorvastatin fed	20 mg/kg
Low	SXSH fed	0.063 g/kg
Medium	SXSH fed	0.126 g/kg
High	SXSH fed	0.252 g/kg
Model-ABX	Antibiotics fed	62.5 μg/mL ampicillin, 62.5 μg/mL metronidazole, 62.5 μg/mL neomycin and 31.25 μg/mL vancomycin
SXSH-ABX	SXSH and Antibiotics fed	0.126 g/kg SXSH, 62.5 μg/mL ampicillin, 62.5 μg/mL metronidazole, 62.5 μg/mL neomycin and 31.25 μg/mL vancomycin

embedding with paraffin. The wax blocks were fixed on a slicer for slicing, and the slices were spread, divided and retrieved in warm water. Finally, the slices were baked in an electric drying oven for 4–6 h, cooled, and stored at room temperature. Then the sections were stained with hematoxylin-eosin (H&E, Wuhan Servicebio Biological Technology Co., Ltd., Wuhan, China) in accordance with the standard protocol to evaluate the severity of myocardial inflammation. The pathological sections were viewed and photographed with a light microscope (Eclipse CI, Nikon Corporation, Tokyo, Japan) and an EVOS M7000 imaging system (Thermo Fisher Scientific, USA).

Serum biochemical measurement

The activities of the antioxidant superoxide dismutase (SOD), malondialdehyde (MDA), and lactate dehydrogenase (LDH) in the rat's serum were detected with corresponding kits (Nanjing Jiancheng Institute of Biotechnology, Nanjing, China). The activity of creatine kinase isoenzymes (CK-MB) was determined with Enzyme-linked immunosorbent assay (ELISA) kits (Lanpai Biological Technology Co., Ltd., Shanghai, China). All the procedures were performed according to the manufacturer's instructions.

Gut microbiota analysis

The fecal samples of each group were freshly collected after 3, 7, and 14 days of treatment, snap-frozen at −80 °C. The genome DNA was extracted and purified according to previous study (Wei et al. 2022). The 16S V4 region (primers 515 F: 5′-GTGCCAAGCMGCCGCGGTAA-3′ and 806 R: 5′-GGACTA CHVGGGTWTCTAAT-3′) were amplified and paired-end sequenced on an Illumina HiSeq platform (Illumina, San Diego, CA, USA) according to the standard protocols by Novogene Technology Co. Ltd. (Beijing, China). Sequences were quality-filtered and clustered by operational taxonomic units (OTUs) according to 97% similarity according to Zhao et al. (2021). Alpha diversity of Shannon index and beta diversity of Principal Coordinate Analysis (PCoA) were performed using QIIME and R package. Taxonomic annotation was performed for each sequence using RDP classifier algorithm (http://rdp.cme.msu.edu/), compared to the Silva database.

Untargeted metabolomics

To investigate affected metabolites by SXSH treatment, 100 µL of each serum sample was added to 400 µL extraction solution containing internal standard (L-2-chlorophenylalanine, 2 µg/mL) and incubated at −20 °C for 30 min. Following centrifugation, nitrogen blowing and ultrasonic extraction, 10 or 20 µL of sample were injected through a Waters BEH C8 reverse-phase column (1.8 µm, 100 × 2.1 mm) in the Thermo Fisher UHPLC-Q Exactive HF-X system. The mobile phase was water-acetonitrile (95:5, v/v) (A) and acetonitrile-isopropanol-water (47.5:47.5:5, v/v/v) (B) following with 0.4 mL/min to 0.6 mL/min flow rate. The analysis was carried with elution gradient as follows: 0 min, 0% B; 3.5 min, 24.5% B; 5 min, 65% B; 5.5 min, 100% B; 7.4 min, 100% B; 7.6 min, 51.5% B; 7.8–10 min, 0% B.

Information-dependent tandem mass spectrometry (MS/MS) spectra were obtained in LC-MS/MS experiments using TripleTOF 6500+ mass spectrometry (ABSciex, Foster City, CA, USA). The LC-MS/MS raw data were processed using the R package and ropls (Version1.6.2, http://bioconductor.org/packages/release/bioc/html/ropls.html). The Human Metabolome Database (HMDB, www.hmdb.ca), METLIN metabolite database (metlin.scripps.edu) and other databases were used for more reliable metabolite identification. Significantly enriched metabolites were identified by Kruskal-Wallis H test. Specific metabolites enriched in the SXSH group compared to Sham or Model with p values < 0.05 were considered statistically significant.

Statistical analysis

All analyses were performed using SPSS statistical software (version 20.0, SPSS Inc., Chicago, IL, USA). Data are presented as mean ± SD. Two-sided Student's t-test was used to compare between the two groups. One-way ANOVA with Tukey's *post hoc* test or a Kruskal-Wallis test followed by Dunn's multiple comparison was used for comparisons among multiple groups. p Values < 0.05 were considered statistically significant for *in vivo* animal studies. GraphPad Prism 8.0 (GraphPad Software Inc., La Jolla, CA, USA) was used for the graphical work.

Results

SXSH protects cardiac function after AMI

Different doses of SXSH were administered to rats orally for 3, 7, and 14 days after AMI (Figure 1(A)). The EF, FS, and hemodynamic parameters AV of the Model group that underwent LAD ligation decreased markedly after 3 days ($p < 0.01$, $p < 0.05$, vs. Sham). The administration of low, medium, and high doses of SXSH for 7 and 14 days could significantly increase the echocardiographic indexes, especially 14 days' medium dose of SXSH treatment increase EF (78.22%), FS (109.07%), and AV (21.62%) ($p < 0.01$, $p < 0.05$, vs. Model) (Figure 1(B–F)). Pathological analysis of the H&E-stained myocardial tissues revealed that the left ventricular wall of the AMI rats was thinned and presented an increased amount of damaged myocardial cells as the number of days increased, leading to severe inflammatory infiltration at the 14th day (Figure 1(G)). The left ventricular wall was thinned and had a reduced the lesion area indicating inflammatory infiltration after different doses of SXSH for 3, 7, and 14 days-treatment. The serum activities of cardiac damage markers LDH and CK-MB were elevated at the 3rd day after AMI ($p < 0.01$, $p < 0.05$, vs. Sham), and the oral administration of medium dose SXSH for 7 days could effectively decrease LDH (33.11%) and CK-MB (33.57%) serum activities ($p < 0.01$, vs. Model), and 8.49% and 10.79% for 14 days, respectively (Figure 1(H-1)). Thus, the administration of SXSH, especially at medium dose concentrations, for 7 and 14 days, can improve the cardiac function and promote the morphological recovery of ischemic myocardial tissue.

SXSH modulates gut microbiota post AMI

Compared to the Sham group, the Shannon index-based alpha diversity of gut microbiota in rats with AMI tends to decrease after 14 days-treatment. What's more, the Shannon index was decreased after 3, 7 days of SXSH intervention in rats with AMI, and increased after 14 days-intervention. Compared to the Model group, the medium-dose SXSH treatment elevated 78.57% of Shannon index at the 14th day (Figure 2(A)). The PCoA analysis for medium dose treatment indicated that the microbial

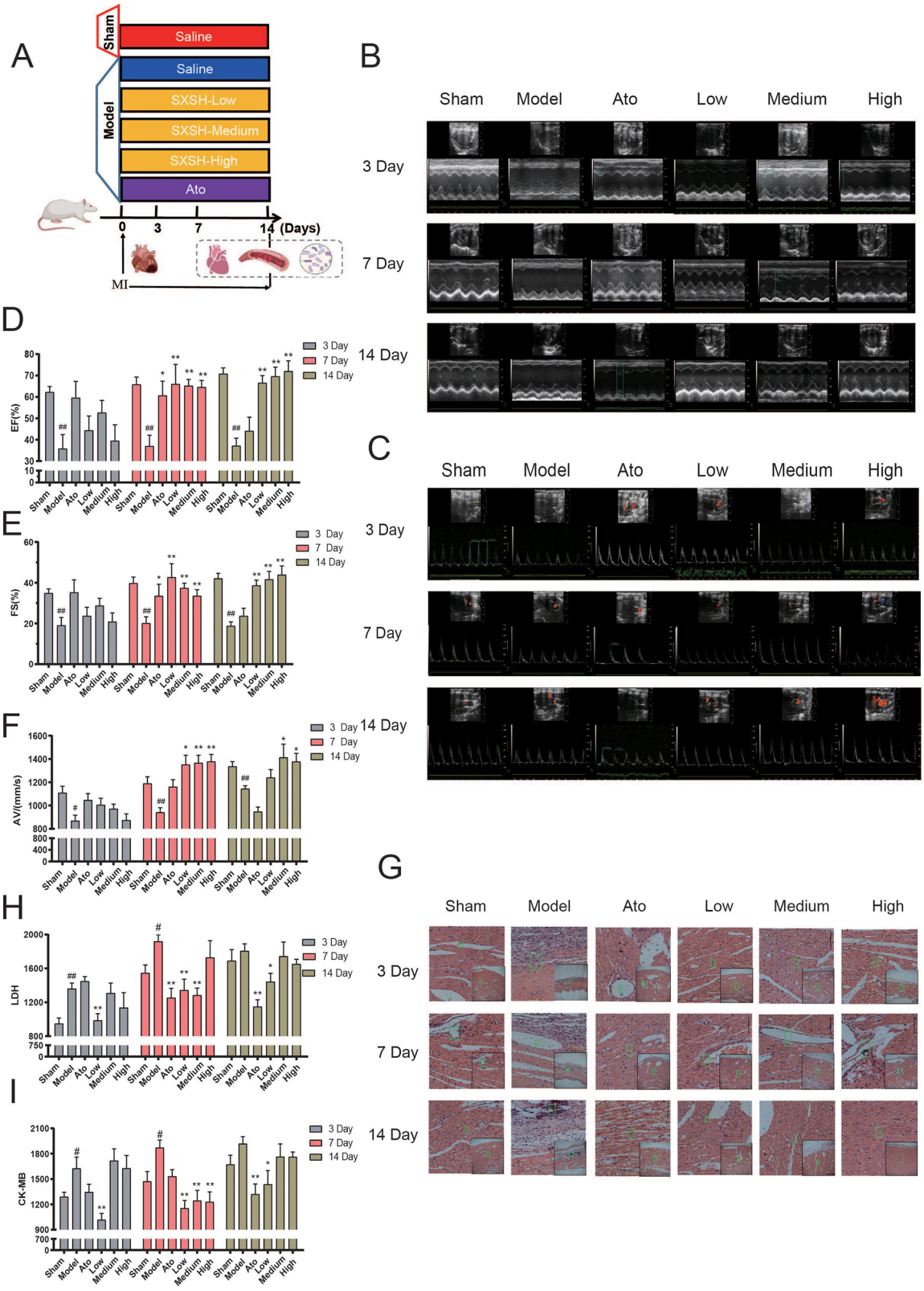

Figure 1. SXSH protects cardiac function after AMI. (A) The schematic diagram for SXSH administration in rats after AMI. (B) Representative parasternal long-axis views and M-mode images. (C) Representative color Doppler imaging of the cardiac outflow tract and blood flow velocity. (D-F) The quantization charts corresponding to EF, FS, and AV. (G) Representative heart pictures of H&E staining (scale bar equals 100 μm). serum activities of (H) LDH, and (I) CK-MB. $^{\#}p < 0.05$, $^{\#\#}p < 0.01$ vs. Sham and $^{*}p < 0.05$, $^{**}p < 0.01$ vs. Model.

community of Model samples was not significantly separate from that of Sham samples at the 3rd, 7th day post AMI, while distinct clustering of microbiota composition for each group was revealed after 14 days-treatment (Figure 2(B)). The gut microbial community at operational taxonomic unit (OTU) level was analyzed and the species biomarkers were figured out after

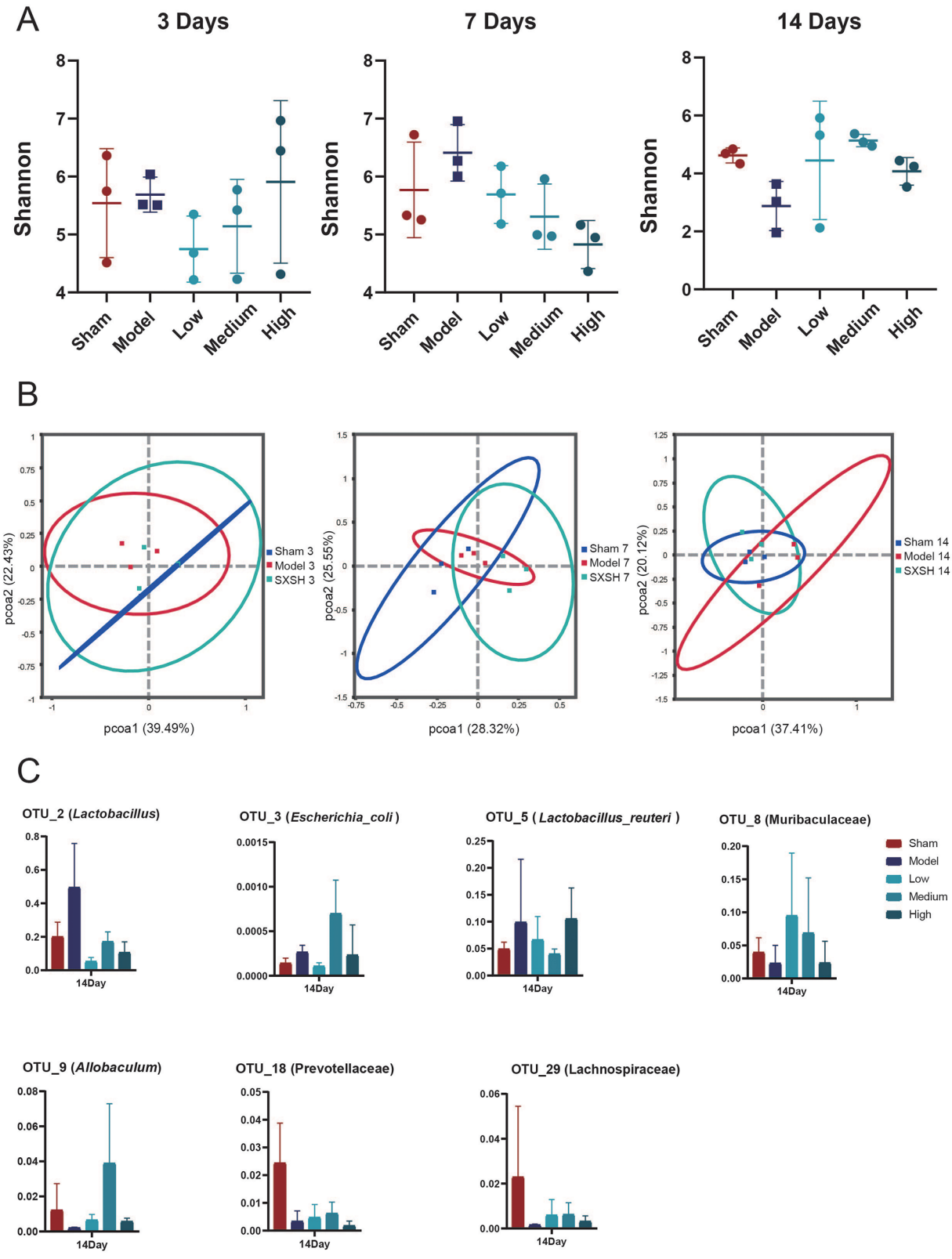

Figure 2. SXSH modulates gut microbiota post AMI. (A) Alpha diversity of Shannon index in each group. (B) Beta diversity of Bray Curtis-based PCoA of medium dose SXSH groups for 3 days, 7 days, and 14 days administration. (C) Statistical analysis of representative OTUs among different groups after 14 days administration.

14 days-intervention with medium dose SXSH. Compared with the Sham group, OTU_2 (*g_Lactobacillus*), OTU_3 (*s_Escherichia_coli*), OTU_5 (*s_Lactobacillus_reuteri*) were upregulated in the intestine of the Model group of AMI rats, while OTU_8 (f_Muribaculaceae), OTU_9 (*g_Allobaculum*), OTU_18 (f_Prevotellaceae), OTU_29 (f_Lachnospiraceae) were downregulated. Among these bacteria, OTU_8 (f_Muribaculaceae) (199.71%), OTU_9 (*g_Allobaculum*) (1744.09%) were upregulated after 14 days- medium dose (0.126 g/kg) of SXSH administration, while OTU_2 (*g_Lactobacillus*) (65.51%), OTU_5 (*s_Lactobacillus reuteri*) (59.68%) were

Table 2. Changes in gut microbiota on different days.

		3 Day		7 Day		14 Day	
OTU	Bacteria	S-M	D-M	S-M	D-M	S-M	D-M
OTU_3	s__Escherichia_coli	+	+	+	+		
OTU_7	s__Lactobacillus_intestinalis	+	+				+
OTU_9	g__Allobaculum	+		+			+
OTU_24	g__Romboutsia	+				−	
OTU_6	f__Muribaculaceae	+	+	+	−	−	
OTU_1	s__Lactobacillus_gasseri	−	−	+	+	+	+
OTU_26	f__Muribaculaceae	−					
OTU_17	s__Enterococcus_durans	−	−	+			
OTU_4	g__unidentified_Prevotellaceae	−	−				
OTU_12	f__Muribaculaceae	−	−				
OTU_2	g__Lactobacillus		+		+	−	−
OTU_10	f__Muribaculaceae		+	−			
OTU_58	g__Bacteroides		−				
OTU_11	f__Muribaculaceae			−	−		
OTU_8	f__Muribaculaceae			−			+
OTU_43	f__Ruminococcaceae			−	−		
OTU_22	s__Akkermansia_muciniphila			−			
OTU_29	f__Lachnospiraceae				+	+	
OTU_18	f__Prevotellaceae				+	+	
OTU_25	g__unidentified_Ruminococcaceae				−		
OTU_27	f__Muribaculaceae				−		
OTU_20	f__Prevotellaceae					+	
OTU_13	f__Muribaculaceae					+	
OTU_5	s__Lactobacillus_reuteri					−	−
OTU_55	f__Ruminococcaceae					−	
OTU_15	o__Bacteroidales						+
OTU_23	f__Prevotellaceae						−
OTU_39	f__Muribaculaceae						−
OTU_84	f__Muribaculaceae						−

"S-M" represents Sham vs. Model; "D-M" represents SXSH administration group vs. Model; "+" represents top 5 upregulated bacteria; "−" represents top 5 downregulated bacteria.

downregulated (Figure 2(C) and Table 2). Collectively, 0.126 g/kg of SXSH administration for 14 days can significantly modulate the gut microbiota composition of AMI rats.

Antibiotics induced dysbacteriosis interferes cardiac protective effect of SXSH

To determine the importance of SXSH in modulating gut microbiota during the treatment of AMI, we administered antibiotics to rats orally 7 days before AMI (Figure 3(A)). The echocardiographic examination indicated that ABX treatment did not affect the cardiac function of Model samples compared with the ABX-free Model samples (Figure 3(B–E)). Compared with the 0.126 g/kg of SXSH administration for 14 days (SXSH group), ABX treatment (SXSH-ABX) abolished its cardiac protection effects with 37.48% lower EF and 42.67% lower FS ($p < 0.001$), and 33.76% lower AV ($p < 0.01$) (Figure 3(C–E)). The histopathological analysis of H&E staining revealed that the SXSH-ABX treatment samples had damaged myocardial cells, intercellular edema, inflammatory infiltration and apparent thinning of the left ventricular wall compared with the SXSH group (Figure 3(F)). The extent of myocardial oxidative and infarct damage was also assessed under the condition of antibiotic-induced dysbiosis (Figure 3(G–J)). Compared with the Sham group, the serum activity of SOD was significantly lower ($p < 0.05$), the serum activities of MDA and LDH were significantly higher ($p < 0.01$, $p < 0.05$) after AMI, and MDA was reduced after SXSH intervention ($p < 0.01$). ABX treatment (SXSH-ABX) did not remarkably affect the SOD, MDA, LDH, and CK-MB activities compared with the SXSH samples.

Global overview of serum metabolites altered by SXSH

To investigate the global metabolism variations of the bio-candidates by SXSH, we conducted an untargeted metabonomic analysis. A total of 689 compounds were identified through database comparison and matching. A remarkable separation between the Sham and Model samples was also observed in the supervised orthogonal partial least squares discriminate analysis (OPLS-DA) score plot, as well as a significant separation of samples between Sham and Model groups in the principal component analysis (PCA) score chart (Figure 4(A,B)).

Compared with the Sham group, the Model group showed 52 differential metabolites were detected in the pos mode, and 53 differential metabolites in the neg mode (Figure 4(C)). The SXSH group showed better dispersion from the Model group and tended to approach the Sham group (Figure 4(D)). A total of 35 difference compounds were obtained with the requirement of variable importance in the projection (VIP) > 1, $p < 0.05$ after SXSH administration (vs. Model; Table 3). KEGG enrichment analysis reflected that SXSH-affected compounds were involved in the choline metabolism in cancer, glycerophospholipid metabolism, D-glutamine and D-glutamate metabolism, retrograde endocannabinoid signalling, bile secretion, and steroid hormone biosynthesis (Figure 4(E)).

Identification of the serum metabolic biomarker associated with cardiac traits

To further identify key metabolites associated with SXSH-mediated alteration of metabolomics, correlation analysis of pharmacodynamic indicators and metabolites was conducted. The alterations in SXSH-regulated metabolites in Table 3 showed that SXSH administration downregulated the abundance of metabolites, such as 2-nonen-1-ol (2.40%), mammeigin (4.43%), D-pipecolic acid (1.62%), 2-*n*-tetrahydrothiophenecarboxylic acid (THTC, 1.73%), estrone (8.33%), lysophosphatidylcholine (lysoPC (O-18:0), 4.61%), lysophosphatidylethanolamine (lysoPE (22:0/0:0), 3.89%), phosphatidylcholine (PC (19:0/0:0), 4.68%), and upregulated the abundance of metabolites, such as bimatoprost (57.14%). Spearman correlation analysis indicated that the abundance of PC [16:0/20:4(5Z,8Z,11Z,14Z)] and PE-NMe [18:0/22:6(4Z,7Z,10Z,13Z,16Z,19Z)] positively correlated with the levels of EF, and FS, while the abundance of THTC showed opposite results. Moreover, the abundance of lysoPC (20:0), lysoPC (P-18:0), and lysoPC [20:2(11Z,14Z)] positively correlated with the activity of MDA (Figure 5(A)). Based on VIP value > 1, total 9 significantly altered metabolites were observed following ABX administration, including upregulation of THTC and 2-nonen-1-ol, downregulation of bimatoprost, mammeigin, D-pipecolic acid, estrone, lysoPC (O-18:0), lysoPE (22:0/0:0), and PC (19:0/0:0) (Figure 5(B)).

Discussion

SXSH contains more than a dozen kinds of Chinese herbs with complex ingredients, from which 38 chemical constituents and six anti-inflammatory and antioxidant compounds have been identified (Liu J et al. 2020). Among them, gallic acid has antioxidant and myocardial protective effects (Badavi et al. 2014; Kongpichitchoke et al. 2016). Eugenol can play a role in

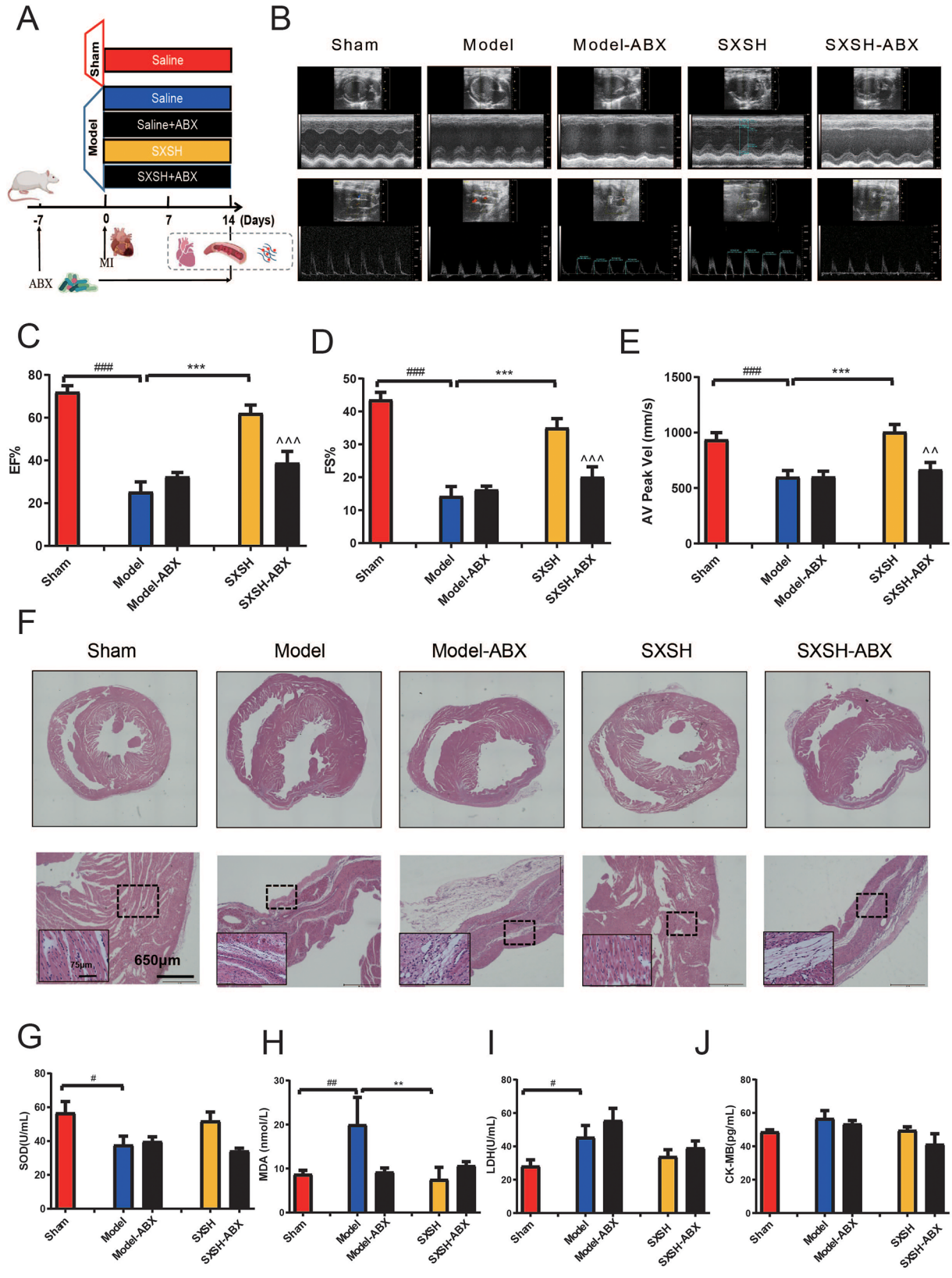

Figure 3. Antibiotics induced dysbacteriosis interferes cardiac protective effect of SXSH. (A) The schematic diagram for SXSH and ABX administration in AMI rats. (B) Representative parasternal long-axis views and M-mode images, and color Doppler imaging of the cardiac outflow tract and blood flow velocity. (C-E) The quantization charts corresponding to EF, FS, and AV. (F) Representative heart pictures of H&E staining [scale bar equals 3000 μm (top), 650 μm and 75 μm (bottom)]. serum activities of (G) SOD, (H) MDA, (I) LDH, and (J) CK-MB. $^{\#}p<0.05$, $^{\#\#}p<0.01$, $^{\#\#\#}p<0.001$ vs. Sham, $^{**}p<0.01$, $^{***}p<0.001$ vs. Model, and $^{\wedge\wedge}p<0.01$, $^{\wedge\wedge\wedge}p<0.001$ vs. SXSH.

protecting rat transplanted hearts from ischemia/reperfusion injury by inhibiting inflammation and apoptosis (Feng et al. 2018). Cinnamon acid combined with licorice and Chuanxiong can prevent myocardial ischemia/reperfusion injury in rats (Gao Y et al. 2015). The above-mentioned chemical components provide the pharmacodynamic material basis for the clinical use of

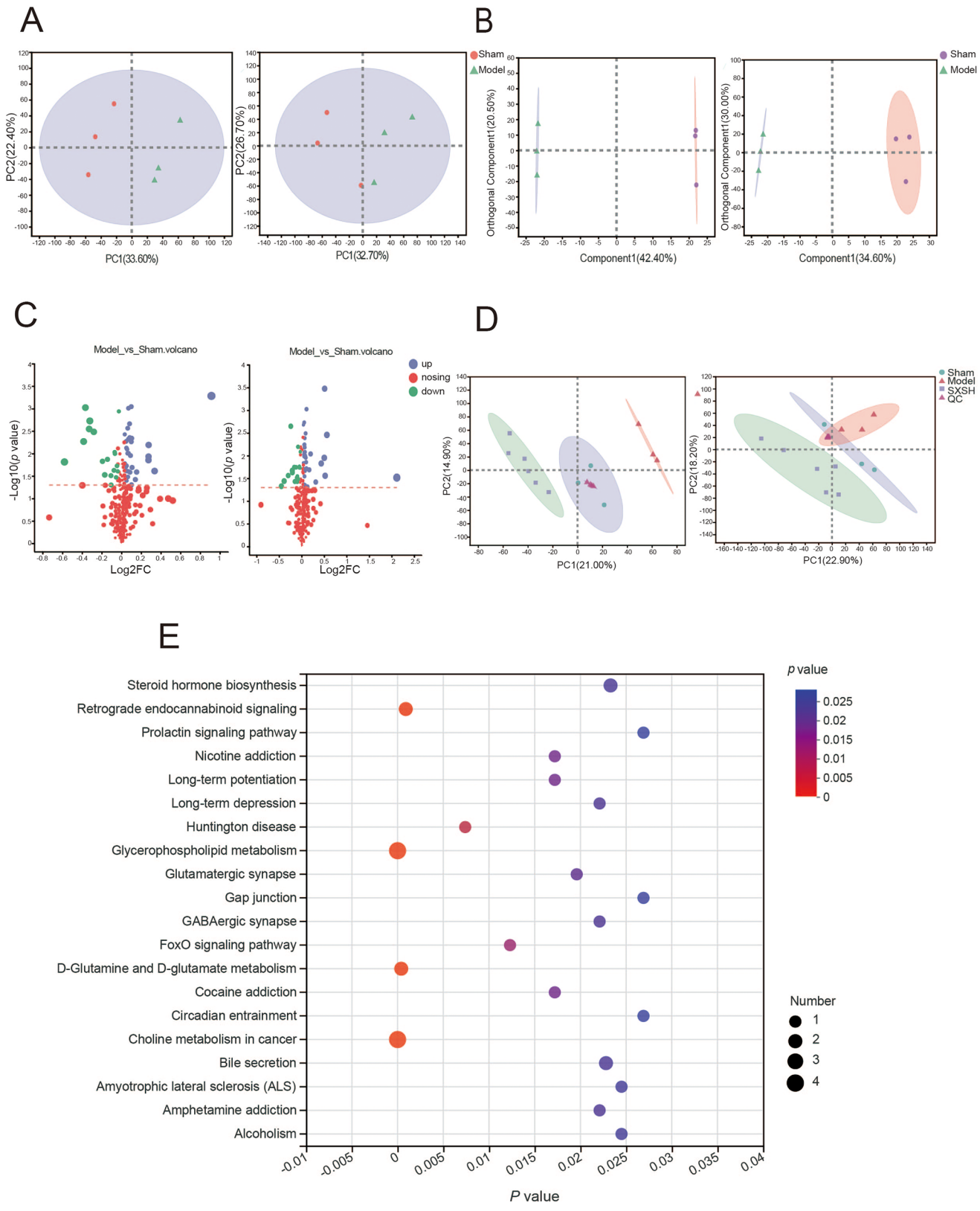

Figure 4. Circulating metabolomics for the quantification of metabolites among different groups. (A) The PCA score plots between Sham and Model in positive ion mode [$R^2Xp1 = 0.336$, $R^2Xp2 = 0.224$] and negative ion mode [$R^2Xp1 = 0.327$, $R^2Xp2 = 0.267$]. (B) The OPLS-DA score plots between Sham and Model in positive ion mode [$R^2X = 0.422$, $R^2Y = 0.973$, $Q^2 = 0.859$] and negative ion mode [$R^2X = 0.346$, $R^2Y = 0.912$, $Q^2 = 0.695$]. (C) Volcano plot showing the differentially accumulated and significantly changed metabolites in Model group compared to Sham. (D) The PCA score plots between Sham, Model, and SXSH in positive ion mode [$R^2Xp1 = 0.21$, $R^2Xp2 = 0.149$, $R^2Xp3 = 0.116$, $R^2Xp4 = 0.112$] and negative ion mode [$R^2Xp1 = 0.229$, $R^2Xp2 = 0.182$, $R^2Xp3 = 0.119$]. (E) Pathway enrichment based on altered metabolites.

Table 3. SXSH administration regulates differential metabolites

Number	Metabolite	M/Z	Formula	Retention time	
1	2-Nonen-1-ol	302.3	$C_9H_{18}O$	6.02135	↓
2	D-Pipecolic acid	130.0	$C_6H_{11}NO_2$	0.479767	↓
3	THTC	150.0	$C_5H_8O_2S$	0.77105	↓
4	LysoPC(P-18:0)	508.3	$C_{26}H_{54}NO_6P$	6.56685	↓
5	Enantio-PAF C-16	524.3	$C_{26}H_{54}NO_7P$	6.589167	↓
6	PC(16:0/20:4(5*Z*, 8*Z*, 11*Z*, 14*Z*))	804.5	$C_{44}H_{80}NO_8P$	7.334717	↑
7	*ent*-7-Oxo-8(14), 15-pimaradien-19-oic acid	361.1	$C_{20}H_{28}O_3$	4.348117	↑
8	*N*, *N*-Dimethyl-Safingol	330.3	$C_{20}H_{43}NO_2$	6.0664	↓
9	Choline	104.1	$C_5H_{13}NO$	6.626383	↓
10	LysoPC(20:2(11*Z*, 14*Z*))	530.3	$C_{28}H_{54}NO_7P$	6.626383	↓
11	LysoPE(22:0/0:0)	560.3	$C_{27}H_{56}NO_7P$	6.6935	↓
12	PC(19:0/0:0)	538.3	$C_{27}H_{56}NO_7P$	6.700983	↓
13	PC(22:1(11*Z*)/0:0)	578.4	$C_{30}H_{60}NO_7P$	6.783167	↓
14	PS(DiMe(11, 3)/DiMe(13, 5))	968.5	$C_{50}H_{86}NO_{12}P$	7.665267	↑
15	LysoPC(20:0)	552.4	$C_{28}H_{58}NO_7P$	6.805583	↓
16	Phosphocholine	184.0	$C_5H_{14}NO_4P$	6.559367	↓
17	PC(16:1(9*Z*)/2:0)	536.3	$C_{26}H_{50}NO_8P$	6.133833	↓
18	Tanacetol B	314.2	$C_{17}H_{28}O_4$	5.885183	↓
19	Estrone	315.1	$C_{18}H_{22}O_2$	5.7404	↓
20	Assamsaponin B	659.2	$C_{61}H_{92}O_{28}$	3.487067	↑
21	*N*-Acetyltyramine	180.1	$C_{10}H_{13}NO_2$	2.83315	↓
22	Mammeigin	427.1	$C_{25}H_{24}O_5$	0.494817	↓
23	PE-NMe(18:0/22:6(4*Z*, 7*Z*, 10*Z*, 13*Z*, 16*Z*, 19*Z*))	850.5	$C_{46}H_{80}NO_8P$	7.21915	↑
24	Dityrosine	359.1	$C_{18}H_{20}N_2O_6$	3.810883	↓
25	PE(18:1(9*Z*)/0:0)	478.2	$C_{23}H_{46}NO_7P$	6.485583	↓
26	LysoPC(20:0/0:0)	596.3	$C_{28}H_{58}NO_7P$	6.8057	↓
27	PE-NMe2(18:0/20:4(5*Z*, 8*Z*, 11*Z*, 14*Z*))	794.5	$C_{45}H_{82}NO_8P$	7.656367	↑
28	PE-NMe2(16:0/18:1(9*Z*))	766.5	$C_{41}H_{80}NO_8P$	7.3342	↑
29	PE-NMe2(16:0/22:6(4*Z*, 7*Z*, 10*Z*, 13*Z*, 16*Z*, 19*Z*))	790.5	$C_{45}H_{78}NO_8P$	7.21915	↓
30	LysoPC(O-18:0)	554.4	$C_{26}H_{56}NO_6P$	6.78305	↓
31	Daphniphylline	526.4	$C_{32}H_{49}NO_5$	6.569517	↓
32	4-Hydroxydebrisoquine	236.1	$C_{10}H_{13}N_3O$	6.17285	↑
33	Bimatoprost	460.3	$C_{25}H_{37}NO_4$	6.011733	↑
34	(*S*)-5, 7-Dihydroxy-6, 8-dimethylflavanone	329.1	$C_{17}H_{16}O_4$	5.40835	↓
35	L-Glutamate	146.0	$C_5H_9NO_4$	0.588583	↓

"↑" upregulated; "↓" downregulated, vs. Model.

SXSH in the treatment of angina pectoris in coronary artery disease, but the underlying mechanisms of the SXSH formula in treating cardiovascular disease remain unclear. We conducted this study based on previous research to demonstrate the gut microbiota-regulated therapeutic effects of SXSH and identify the targeted microbes and metabolites. We selected atorvastatin as a positive control drug for comparison, the efficacy of which in improving MI has been demonstrated (Schwartz et al. 2001; Huang P et al. 2020). Our results revealed that atorvastatin elevated EF, FS levels, and reduced LDH and CK-MB activity after 14 days-treatment. SXSH was significantly more effective than atorvastatin in terms of ultrasound results, while atorvastatin was more effective than SXSH in terms of improving post-infarction serum enzyme activity, which may be related to the time of administration and the different reference indices. Depletion of the microbes with antibiotics abrogated the anti-AMI effects of SXSH, indicating that the efficacy of SXSH was gut microbiota dependent. Elucidating the mechanism of drug-dependent gut microbiota regulation may provide a theoretical basis for subsequent flora precision treatment for cardiovascular diseases.

Gut microbiota can improve myocardial infarction by regulating lipid metabolism, blood pressure, and apoptosis and through many other ways (Zununi Vahed et al. 2018). In this study, we found a gradual increase in flora diversity and a decrease in diversity in the AMI rats when the duration of SXSH administration increased presumably because the increased gut microbiota was conducive to the cardioprotective effect. Song et al. (2021) detected significant changes in Prevotellaceae and Lachnospiraceae in the gut microbiota at different time points after MI, which is consistent with our findings. The upregulated Prevotellaceae and *Allobaculum* are associated with the alleviation of cardiotoxicity (Chen Y, Liu, et al. 2022; Huang J et al. 2022). Specifically, *Allobaculum* is involved in regulating intestinal ANGPTLT4 expression in mice treated with a high-fat diet (Zheng et al. 2021). As a probiotic, *Lactobacillus intestinalis* is involved in regulating the immune system (Wu et al. 2020), which is also enriched by SXSH treatment. The Firmicutes/Bacteroidota ratio and the abundance of Lachnospiraceae, Rikenellaceae, Prevotellaceae, *Streptococcus*, *Romboutsia*, *Roseburia*, and *Lactobacillus* are reported to be associated with cardiovascular risk factors (Serena et al. 2018; Gao F et al. 2019; Toya et al. 2020; Zhang et al. 2020). Possibly, the pharmacological effect of SXSH is also the result of the interaction of accumulated beneficial microbes.

Untargeted metabolomics has led to many discoveries on microbiota-dependent metabolic pathways and metabolites associated with the host disease (Han et al. 2021). Thirty-five metabolites regulated by SXSH and involved in multiple metabolic pathways might play a role in the treatment of AMI. For example, choline and phosphocholine, which are associated with the choline metabolic pathway, are downregulated. Meanwhile, KEGG enrichment analysis has shown that SXSH-affected compounds can be involved in choline metabolism. Both metabolites are associated with an increased risk of major adverse cardiovascular events (Wang Z et al. 2011; Tang et al. 2013; de Vries et al. 2021). In addition, SXSH can downregulate dityrosine and L-glutamate levels (Yang et al. 2017), which are both correlated with cardiovascular disease severity. Moreover, the metabolites lysoPC and PC, which are significantly correlated with EF, FS, MDA, and other pharmacodynamic indicators, are downregulated by SXSH. Studies have shown that elevated levels of specific PC are a feature of cardiovascular risk and mortality (Liu H et al. 2019). LysoPC is a risk factor for atherosclerosis and is related to lipid homeostasis (Wang Y et al. 2021). Additionally, the crucial component of oxidized low-density lipoprotein is lysoPC, a robust pro-inflammatory mediator. A close correlation exists between myocardial lysoPC and plasma troponin I levels, with lysoPC treatment of cardiomyocytes leading to cell death in a dose- and time-dependent manner (Oestvang et al. 2011; Huang JP et al. 2016). Furthermore, clinical studies have identified different rates of lysophospholipid metabolites (mainly lysoPC and lysoPE) as predictive markers for STEMI (Chorell et al. 2020). The active ingredients of SXSH have also been investigated. Kaempferol can improve the perturbation of metabolites related to tryptophan, fatty acid, and secondary bile acid metabolism in the intestines of mice (Aa et al. 2020). Another active ingredient, asiatic acid, also affects the biosynthesis of metabolites, such as phosphatidylcholine, phosphatidylethanolamine, and phosphatidylserine, and regulates the glycerophospholipid metabolic pathway (Chen S, Huang, et al. 2022). This finding is consistent with our result that SXSH is involved in modulating glycerophospholipid metabolism. However, some studies have shown that asiatic acid is significantly associated with an increase in choline (Songvut et al. 2021), which contradicts the results of the present study. Such an increase may be the result of the synergistic effect of multiple components in the herbal compound.

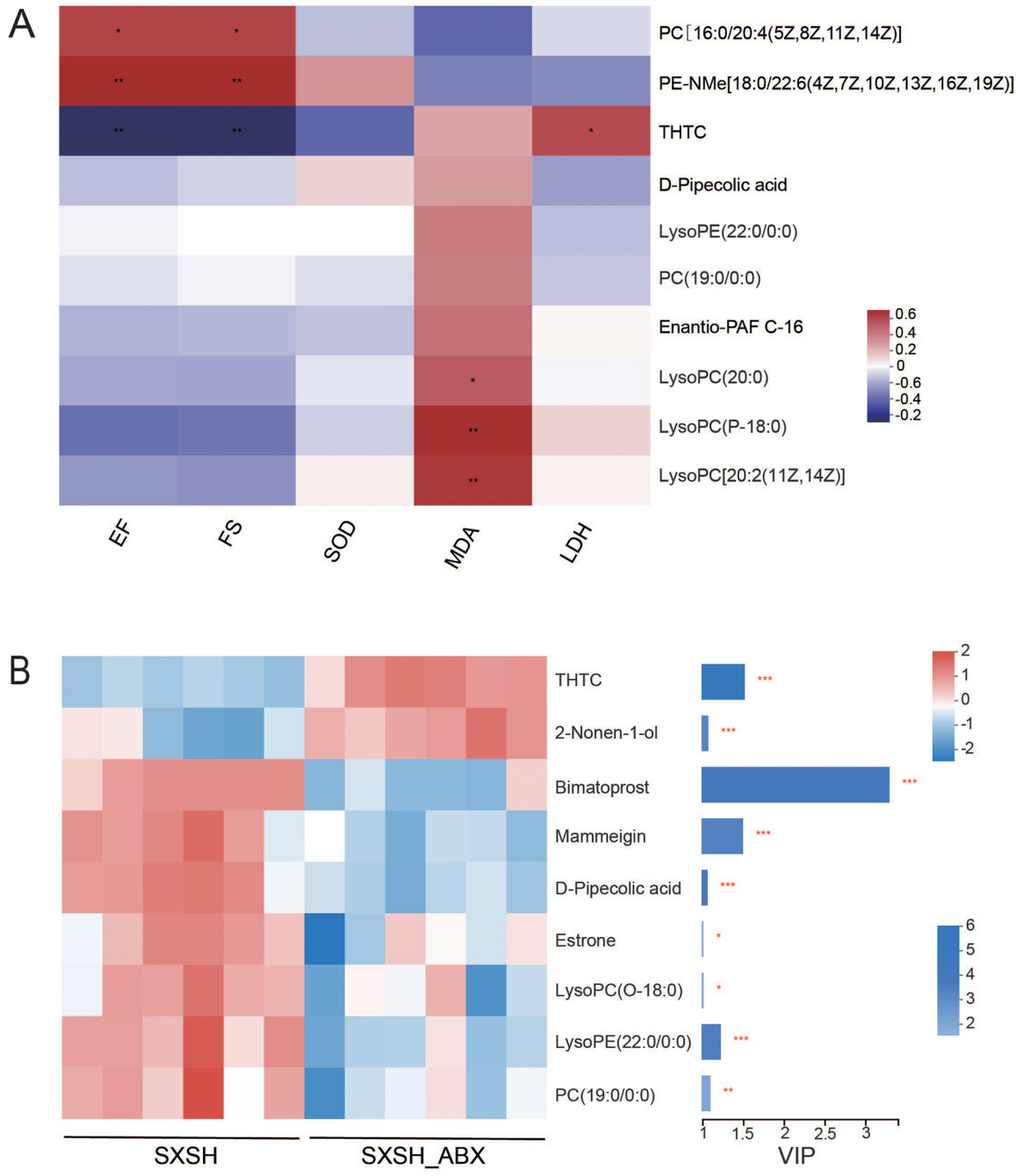

Figure 5. Biomarker analysis and heatmap of identified marker metabolites. (A) Spearman correlation analysis among key efficacy indicators and marker metabolites. (B) Heatmap of selected marker metabolites among SXSH and SXSH-ABX group based on VIP > 1.

Conclusions

SXSH improved cardiac function, slowed down the pathological process of myocardial injury, and reduced CK-MB and LDH values in rats after AMI. Such efficacy was achieved by upregulating the abundance of gut microbiota, including Muribaculaceae, *Allobaculum*, and by downregulating *Lactobacillus*, and metabolite levels (e.g., THTC). Our findings suggest that gut microbiota is an important means for SXSH to protect the heart from damage and provide a theoretical basis for using TCM to investigate cardiovascular disease through the regulation of gut microbes and related metabolites.

Authors' contributions

Prof. XY. Wang: Conceptualization, Project administration. XQ. Zhong: Data curation, Writing- original draft. JY. Yan, X. Wei, T. Xie, and ZJ. Zhang: Methodology. KY. Wang, CY. Sun, W. Chen, and JM. Zhu: Visualization, Software. X. Zhao: Writing-review & editing. All authors read and approved the final manuscript.

Disclosure statement

No potential conflict of interest was reported by the author(s).

Funding

This work was supported by National Key R&D Program of China (2022YFC3500300; 2022YFC3500305; 2018YFC1704500); The Innovation Team and Talents Cultivation Program of National Administration of Traditional Chinese Medicine (ZYYCXTD-C-202009).

Data availability statement

The data generated for 16S rRNA gene profiling of bacteria are available in the NCBI repository with project accession number PRJNA900688.

References

Aa LX, Fei F, Qi Q, Sun RB, Gu SH, Di ZZ, Aa JY, Wang GJ, Liu CX. 2020. Rebalancing of the gut flora and microbial metabolism is responsible for the anti-arthritis effect of kaempferol. Acta Pharmacol Sin. 41(1):73–81. doi: 10.1038/s41401-019-0279-8.

Badavi M, Sadeghi N, Dianat M, Samarbafzadeh A. 2014. Effects of gallic acid and cyclosporine a on antioxidant capacity and cardiac markers of rat isolated heart after ischemia/reperfusion. Iran Red Crescent Med J. 16(6):e16424. doi: 10.5812/ircmj.16424.

Chen D, Liu J, Chen H, Guan Y, Zhu Q, Su D. 2000. Effect of Shenxiang Suhe pill on rats with myocardial ischemia. Tradi Chinese Drug Res Clin Pharmacol. 11:86–88. (in Chinese)

Chen S, Huang Y, Su H, Zhu W, Wei Y, Long Y, Shi Y, Wei J. 2022. The integrated analysis of transcriptomics and metabolomics unveils the therapeutical effect of asiatic acid on alcoholic hepatitis in rats. Inflammation. 45(4):1780–1799. doi: 10.1007/s10753-022-01660-x.

Chen Y, Liu Y, Wang Y, Chen X, Wang C, Chen X, Yuan X, Liu L, Yang J, Zhou X. 2022. Prevotellaceae produces butyrate to alleviate PD-1/PD-L1 inhibitor-related cardiotoxicity via PPARα-CYP4X1 axis in colonic macrophages. J Exp Clin Cancer Res. 41(1):1. doi: 10.1186/s13046-021-02201-4.

Chinese Pharmacopoeia Commission. 2020. Pharmacopoeia of the People's Republic of China. Vol 1. Beijing (China): Ministry of Health of the People's Republic of China; p. 1424.

Chorell E, Olsson T, Jansson JH, Wennberg P. 2020. Lysophospholipids as predictive markers of ST-elevation myocardial infarction (STEMI) and non-ST-elevation myocardial infarction (NSTEMI). Metabolites. 11(1):25. doi: 10.3390/metabo11010025.

de Vries MR, Ewing MM, de Jong RCM, MacArthur MR, Karper JC, Peters EAB, Nordzell M, Karabina SAP, Sexton D, Dahlbom I, et al. 2021. Identification of IgG1 isotype phosphorylcholine antibodies for the treatment of inflammatory cardiovascular diseases. J Intern Med. 290(1):141–156. doi: 10.1111/joim.13234.

Feng W, Jin L, Xie Q, Huang L, Jiang Z, Ji Y, Li C, Yang L, Wang D. 2018. Eugenol protects the transplanted heart against ischemia/reperfusion injury in rats by inhibiting the inflammatory response and apoptosis. Exp Ther Med. 16(4):3464–3470. doi: 10.3892/etm.2018.6598.

Forte E, Perkins B, Sintou A, Kalkat HS, Papanikolaou A, Jenkins C, Alsubaie M, Chowdhury RA, Duffy TM, Skelly DA, et al. 2021. Cross-priming dendritic cells exacerbate immunopathology after ischemic tissue damage in the heart. Circulation. 143(8):821–836. doi: 10.1161/CIRCULATIONAHA.120.044581.

Gao F, Lv YW, Long J, Chen JM, He JM, Ruan XZ, Zhu HB. 2019. Butyrate improves the metabolic disorder and gut microbiome dysbiosis in mice induced by a high-fat diet. Front Pharmacol. 10:1040. doi: 10.3389/fphar.2019.01040.

Gao Y, Hao J, Zhang H, Qian G, Jiang R, Hu J, Wang J, Lei Z, Zhao G. 2015. Protective effect of the combinations of glycyrrhizic, ferulic and cinnamic acid pretreatment on myocardial ischemia-reperfusion injury in rats. Exp Ther Med. 9(2):435–445. doi: 10.3892/etm.2014.2134.

Gelfand EV, Cannon CP. 2007. Myocardial infarction: contemporary management strategies. J Intern Med. 262(1):59–77. doi: 10.1111/j.1365-2796.2007.01790.x.

Gong P, Li Y, Yao C, Guo H, Hwang H, Liu X, Xu Y, Wang X. 2017. Traditional Chinese medicine on the treatment of coronary heart disease in recent 20 years. J Altern Complement Med. 23(9):659–666. doi: 10.1089/acm.2016.0420.

Han S, Van Treuren W, Fischer CR, Merrill BD, DeFelice BC, Sanchez JM, Higginbottom SK, Guthrie L, Fall LA, Dodd D, et al. 2021. A metabolomics pipeline for the mechanistic interrogation of the gut microbiome. Nature. 595(7867):415–420. doi: 10.1038/s41586-021-03707-9.

Huang J, Wei S, Jiang C, Xiao Z, Liu J, Peng W, Zhang B, Li W. 2022. Involvement of abnormal gut microbiota composition and function in doxorubicin-induced cardiotoxicity. Front Cell Infect Microbiol. 12:808837. doi: 10.3389/fcimb.2022.808837.

Huang JP, Cheng ML, Wang CH, Shiao MS, Chen JK, Hung LM. 2016. High-fructose and high-fat feeding correspondingly lead to the development of lysoPC-associated apoptotic cardiomyopathy and adrenergic signaling-related cardiac hypertrophy. Int J Cardiol. 215:65–76. doi: 10.1016/j.ijcard.2016.03.239.

Huang P, Wang L, Li Q, Tian X, Xu J, Xu J, Xiong Y, Chen G, Qian H, Jin C, et al. 2020. Atorvastatin enhances the therapeutic efficacy of mesenchymal stem cells-derived exosomes in acute myocardial infarction via up-regulating long non-coding RNA H19. Cardiovasc Res. 116(2):353–367. doi: 10.1093/cvr/cvz139.

Kongpichitchoke T, Chiu MT, Huang TC, Hsu JL. 2016. Gallic acid content in Taiwanese teas at different degrees of fermentation and its antioxidant activity by inhibiting PKCδ activation: in vitro and in silico studies. Molecules. 21(10):1346. doi: 10.3390/molecules21101346.

Kwun JS, Kang SH, Lee HJ, Park HK, Lee WJ, Yoon CH, Suh JW, Cho YS, Youn TJ, Chae IH. 2020. Comparison of thrombus, gut, and oral microbiomes in Korean patients with ST-elevation myocardial infarction: a case-control study. Exp Mol Med. 52(12):2069–2079. doi: 10.1038/s12276-020-00543-1.

Liu H, Chen X, Hu X, Niu H, Tian R, Wang H, Pang H, Jiang L, Qiu B, Chen X, et al. 2019. Alterations in the gut microbiome and metabolism with coronary artery disease severity. Microbiome. 7(1):68. doi: 10.1186/s40168-019-0683-9.

Liu J, Wang S, Tan W, Lv B, Dai Y, Wang Y, Zhang Z, Wang X. 2020. Dual-screening of anti-inflammatory and antioxidant active ingredients of Shenxiang Suhe pill and its potential multi-target therapy for coronary heart disease. Biomed Pharmacother. 129:110283. doi: 10.1016/j.biopha.2020.110283.

Nabel EG, Braunwald E. 2012. A tale of coronary artery disease and myocardial infarction. N Engl J Med. 366(1):54–63. doi: 10.1056/NEJMra1112570.

Oestvang J, Anthonsen MW, Johansen B. 2011. lysoPC and PAF trigger arachidonic acid release by divergent signaling mechanisms in monocytes. J Lipids. 2011:532145. doi: 10.1155/2011/532145.

Schwartz GG, Olsson AG, Ezekowitz MD, Ganz P, Oliver MF, Waters D, Zeiher A, Chaitman BR, Leslie S, Stern T. 2001. Effects of atorvastatin on early recurrent ischemic events in acute coronary syndromes: the MIRACL study: a randomized controlled trial. JAMA. 285(13):1711–1718. doi: 10.1001/jama.285.13.1711.

Serena C, Ceperuelo-Mallafré V, Keiran N, Queipo-Ortuño MI, Bernal R, Gomez-Huelgas R, Urpi-Sarda M, Sabater M, Pérez-Brocal V, Andrés-Lacueva C, et al. 2018. Elevated circulating levels of succinate in human obesity are linked to specific gut microbiota. ISME J. 12(7):1642–1657. doi: 10.1038/s41396-018-0068-2.

Shi T, Li D, Long S. 2022. Clinical observation of Shenxiang Suhe pills combined with aspirin in the treatment of type 2 diabetes mellitus complicated with coronary heart disease. China Pharmaceuticals. 31:87–90. (in Chinese)

Song T, Guan X, Wang X, Qu S, Zhang S, Hui W, Men L, Chen X. 2021. Dynamic modulation of gut microbiota improves post-myocardial infarct tissue repair in rats via butyric acid-mediated histone deacetylase inhibition. FASEB J. 35(3):e21385. doi: 10.1096/fj.201903129RRR.

Songvut P, Chariyavilaskul P, Khemawoot P, Tansawat R. 2021. Pharmacokinetics and metabolomics investigation of an orally modified formula of standardized *Centella asiatica* extract in healthy volunteers. Sci Rep. 11(1):12568. doi: 10.1038/s41598-021-92113-2.

Stone GW. 2008. Angioplasty strategies in ST-segment-elevation myocardial infarction: part II: intervention after fibrinolytic therapy, integrated treatment recommendations, and future directions. Circulation. 118(5):552–566. doi: 10.1161/CIRCULATIONAHA.107.739243.

Tang WH, Wang Z, Levison BS, Koeth RA, Britt EB, Fu X, Wu Y, Hazen SL. 2013. Intestinal microbial metabolism of phosphatidylcholine and cardiovascular risk. N Engl J Med. 368(17):1575–1584. doi: 10.1056/NEJMoa1109400.

Toya T, Corban MT, Marrietta E, Horwath IE, Lerman LO, Murray JA, Lerman A. 2020. Coronary artery disease is associated with an altered gut microbiome composition. PLoS One. 15(1):e0227147. doi: 10.1371/journal.pone.0227147.

Wang C, Niimi M, Watanabe T, Wang Y, Liang J, Fan J. 2018. Treatment of atherosclerosis by traditional Chinese medicine: questions and quandaries. Atherosclerosis. 277:136–144. doi: 10.1016/j.atherosclerosis.2018.08.039.

Wang Y, Wu J, Zhu J, Ding C, Xu W, Hao H, Zhang J, Wang G, Cao L. 2021. Ginsenosides regulation of lysophosphatidylcholine profiles underlies the mechanism of Shengmai Yin in attenuating atherosclerosis. J Ethnopharmacol. 277:114223. doi: 10.1016/j.jep.2021.114223.

Wang Z, Klipfell E, Bennett BJ, Koeth R, Levison BS, Dugar B, Feldstein AE, Britt EB, Fu X, Chung YM, et al. 2011. Gut flora metabolism of phosphatidylcholine promotes cardiovascular disease. Nature. 472(7341):57–63. doi: 10.1038/nature09922.

Wei X, Xie T, Zhong X, Zhao X, Wang X. 2022. Effect of Shenxiang Suhe pills on intestinal flora in rats with myocardial infarction. J Tianjin Univ Trad Chinese Med. 41:76–84. (in Chinese)

Wu X, Cao J, Li M, Yao P, Li H, Xu W, Yuan C, Liu J, Wang S, Li P, et al. 2020. An integrated microbiome and metabolomic analysis identifies immunoenhancing features of *Ganoderma lucidum* spores oil in mice. Pharmacol Res. 158:104937. doi: 10.1016/j.phrs.2020.104937.

Yang Y, Zhang H, Yan B, Zhang T, Gao Y, Shi Y, Le G. 2017. Health effects of dietary oxidized tyrosine and dityrosine administration in mice with nutrimetabolomic strategies. J Agric Food Chem. 65(32):6957–6971. doi: 10.1021/acs.jafc.7b02003.

Zhang Z, Liu H, Yu B, Tao H, Li J, Wu Z, Liu G, Yuan C, Guo L, Cui B. 2020. *Lycium barbarum* polysaccharide attenuates myocardial injury in high-fat diet-fed mice through manipulating the gut microbiome and fecal metabolome. Food Res Int. 138(Pt B):109778. doi: 10.1016/j.foodres.2020.109778.

Zhao X, Fu Z, Yao M, Cao Y, Zhu T, Mao R, Huang M, Pang Y, Meng X, Li L, et al. 2021. Mulberry (*Morus alba* L.) leaf polysaccharide ameliorates insulin resistance- and adipose deposition-associated gut microbiota and lipid metabolites in high-fat diet-induced obese mice. Food Sci Nutr. 10(2):617–630. doi: 10.1002/fsn3.2689.

Zheng Z, Lyu W, Ren Y, Li X, Zhao S, Yang H, Xiao Y. 2021. *Allobaculum* involves in the modulation of intestinal ANGPTLT4 expression in mice treated by high-fat diet. Front Nutr. 8:690138. doi: 10.3389/fnut.2021.690138.

Zhou X, Li J, Guo J, Geng B, Ji W, Zhao Q, Li J, Liu X, Liu J, Guo Z, et al. 2018. Gut-dependent microbial translocation induces inflammation and cardiovascular events after ST-elevation myocardial infarction. Microbiome. 6(1):66. doi: 10.1186/s40168-018-0441-4.

Zhu X, Liu H, Yu H, Guo S, Lao Q, Li C. 2016. Experimental study on therapeutic effects of Shenxiang Suhe Pill on cardiovascular diseases. J Zhejiang Sci-Tech Univ (Natural Sciences Edition). 35:630–635. (in Chinese)

Zhuang R, Meng Q, Ma X, Shi S, Gong S, Liu J, Li M, Gu W, Li D, Zhang X, et al. 2022. CD4(+)FoxP3(+)CD73(+) regulatory T cell promotes cardiac healing post-myocardial infarction. Theranostics. 12(6):2707–2721. doi: 10.7150/thno.68437.

Zijlstra F. 2000. Long-term benefit of primary angioplasty compared to thrombolytic therapy for acute myocardial infarction. Eur Heart J. 21(18):1487–1489. doi: 10.1053/euhj.2000.2192.

Zununi Vahed S, Barzegari A, Zuluaga M, Letourneur D, Pavon-Djavid G. 2018. Myocardial infarction and gut microbiota: an incidental connection. Pharmacol Res. 129:308–317. doi: 10.1016/j.phrs.2017.11.008.